SHRINKING CORE MODEL FOR HETEROGENEOUS REACTION- APPLIED TO COAL GASIFICATION IN FLUIDIZED BED

By

S PHANI KIRAN

R080207002

College of Engineering

University of Petroleum & Energy Studies

Dehradun

May, 2009

UPES - Library

DI1095

KIR-2009MT

UNIVERSITY OF PETROLEUM & ENERGY STUDIES
LIBRARY
Acc No.: DI 1095
Date : 22.12.11
New Delhi

SHRINKING CORE MODEL FOR HETEROGENEOUS REACTION - APPLIED TO COAL GASIFICATION IN FLUIDIZED BED

A thesis submitted in partial fulfilment of the requirements for the Degree of

Master of Technology
(Refining & Petrochemical Engineering)

By

S PHANI KIRAN

R080207002

Under the guidance of

Mrs. ROSE HAVILAH PULLAH

Assistant Professor
College of Engineering
University of Petroleum and Energy Studies

Approved

Dr SHRIHARI.

Dean
College of Engineering
University of Petroleum & Energy Studies
Dehradun
May, 2009

UNIVERSITY OF PETROLEUM & ENERGY STUDIES

CERTIFICATE

This is to certify that the work contained in this thesis titled **"SHRINKING CORE MODEL FOR HETEROGENEOUS REACTION RATES - APPLIED TO COAL GASIFICATION IN FLUIDIZED BED"** has been carried out by **S PHANI KIRAN** under my supervision and has not been submitted elsewhere for a degree

P. Rose Havilah
8/5/09

Mrs. ROSE HAVILAH PULLAH

Assistant Professor

Date:

Corporate Office:
Hydrocarbons Education & Research Society
3rd Floor, PHD House,
4/2 Siri Institutional Area
August Kranti Marg, New Delhi - 110 016 India
Ph.: +91-11-41730151-53 Fax : +91-11-41730154

Main Campus:
Energy Acres,
PO Bidholi Via Prem Nagar,
Dehradun - 248 007 (Uttarakhand), India
Ph.: +91-135-2102690-91, 2694201/ 203/ 208
Fax: +91-135-2694204

Regional Centre (NCR) :
SCO, 9-12, Sector-14,
Gurgaon 122 007
(Haryana), India.
Ph: +91-124-4540 300
Fax: +91-124-4540 330

Regional Centre (Rajahmundry):
GIET, NH 5, Velugubanda,
Rajahmundry - 533 294,
East Godavari Dist., (Andhra Pradesh), India
Tel: +91-883-2484811/ 855
Fax: +91-883-2484822

Email: info@upes.ac.in URL : www.upes.ac.in

ACKNOWLEDGEMENT

I would like to take this opportunity to express my most sincere thanks and gratitude to **Mrs. ROSE HAVILAH PULLAH** for guiding me throughout the project. Her guidance has been phenomenal and without her support the realization of this work would not have been possible. She has been inimitable as a supervisor, with infinite moral endurance, character and resolve and has been pivotal in my pursuit toward this goal

I would like to thank **Mr. G SANJAY KUMAR** for his kind support and help throughout the project

I express my sincere thanks to **Dr. R P BADONI** for extending his support in completion of the project

I would also like to take this opportunity to thank my friends K Ram Satish, Research Scholar, Reaction and Transport Processes Laboratory, Department of Chemical Engineering, Indian Institute of Technology Madras and K Sreenath, Master of Science, Department of Chemical Engineering, Indian Institute of Technology Madras for their help with the project. I have thoroughly enjoyed working with them and they provided me with enormous amounts of encouragement and support throughout my project period.

Last, but not least, my immense thanks to the wonderful professors of the College of Engineering. The teaching and cheerful feedback they have imparted during my stay is indispensable. I had so much fun completing my Master of Technology at University of Petroleum and Energy Studies, Dehradun.

ABSTRACT

A new model for solid-gas reaction rates has been proposed. Numerical method developed to compute the heterogeneous reaction rates is discussed. The developed model and the numerical algorithm were tested by studying the effect of various parameters such as Sherwood Number, Thiele Modulus and Grid Size on the solution. After validation of the proposed model for solid-gas reactions, Coal gasification process was chosen to apply the new model for computing reaction rates. Results have been presented for the system considered: combustion and gasification of coal.

A one-dimensional steady state mathematical model and a numerical algorithm have been developed to simulate the coal gasification process in fluidized bed. The model incorporates two phases, the solid and the gas. The new model described in the previous section has been used for computing concentration profiles of gases from a system of heterogeneous reactions and their net production/consumption inside a coal particle. These results were used in model equations of the fluidized bed to compute the flowrates as a function of bed height. The model can predict mass flow rates of components in both the phases. A system of 9 differential equations, derived from mass balances for each phase, at any point along the bed, were solved in MATLAB 6.5 using ode15s solver.

Keywords: Fluidized Bed; Solid-Gas Reactions; Thiele Modulus

TABLE OF CONTENTS

1	**Introduction**	1
	1.1 Coal Gasification	1
	1.2 Chemistry	1
	1.3 Fluidized Bed Gasifier	2
2	**Literature Survey**	3
3	**Objectives of Research**	4
4	**Heterogeneous Reactions**	5
	4.1 Single Reaction – Particle Kinetics	5
	4.1.1 Grid Size	7
	4.1.2 Sherwood Number	9
	4.1.3 Thiele Modulus	11
	4.2 Multiple Reactions	12
5	**Mathematical Model**	15
	5.1 Chemical Reactions	15
	5.2 Model Equations	15
	5.3 Boundary Conditions	18
	5.4 Auxiliary Equations	19
	5.4.1 Gas-Gas Diffusivities	19
	5.4.2 Gas-Solid Diffusivities	19
	5.5 Core Dimension	20
	5.6 Heat and Mass Transfer Coefficients	20
6	**Numerical Solution**	22
	6.1 Choosing Solver	22
	6.2 Discretization	23
	6.3 Basic Description of the Algorithm	24
7	**Results & Discussion**	25
8	**Conclusions & Future Work**	29

	Nomenclature	30
	Bibliography	32
	Appendix	33

LIST OF FIGURES

Fig. 1.	Schematic Diagram of a fluidized bed reactor	2
Fig. 2.	Shrinking Core model for gas-solid reactions	5
Fig. 3.	(a). O_2 Concentration inside a coal particle: Low Grid No.	8
	(b). O_2 Concentration inside a coal particle: High Grid No.	8
Fig. 4.	O_2 Concentration Profile at different Sherwood Number	10
Fig. 5.	O_2 Concentration Profile at different Thiele Modulus	11
Fig. 6.	Concentration profiles of all gases inside the coal particle	12
Fig. 7.	CO_2 concentration at different temperatures	13
Fig. 8.	Program Diagram	24
Fig. 9.	CO_2 flowrate: Comparison of the two methods	25
Fig. 10.	CO flowrate: Comparison of the two methods	26
Fig. 11	O_2 flowrate along the bed height	26
Fig. 12.	Molar composition as a function of bed height.	27
Fig. 13.	(a). Effect of gas phase temperature on gas production rates	28
	(b). Effect of solid phase temperature on gas production rates	28

LIST OF TABLES

Table 1	Grid Size vs Correlation Coefficient (r^2)	9
Table 2	N1 vs Flux ratio	10
Table 3	Chemical Reactions	15
Table 4	Gas components indices	18
Table 5	Boundary Conditions	18
Table 6	Program run time for different solvers	22

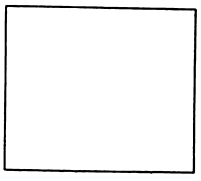

1.1 Coal Gasification

Coal gasification is a clean coal technology that presents good prospects for coal use, mainly for producing electricity with a high coal conversion efficiency and low environmental impact. In this process, coal is converted into carbon monoxide and hydrogen by treating it at high temperatures with a controlled amount of oxygen and steam. The resulting gas mixture is called synthesis gas or syngas and is itself a fuel. The advantage of gasification is that using the syngas is more efficient than direct combustion of the original fuel; more of the energy contained in the fuel is extracted. Syngas may be burned directly in internal combustion engines, used to produce methanol and hydrogen, or converted via the Fischer-Tropsch process into synthetic fuel.

Coal gasification offers one of the most clean and versatile ways to convert the energy contained in coal into electricity, hydrogen, and other sources of power.

1.2 Chemistry

The primary desired reactions in a gasification process are combustion of coal (with oxygen) and gasification of coal (with steam). Energy produced from former reaction (exothermic) is used in for the latter (exothermic).

The *combustion* process occurs as the volatile products and some of the char reacts with oxygen to form carbon dioxide and carbon monoxide, which provides heat for the subsequent gasification reactions.

$$C + \frac{1}{2} O_2 \rightarrow CO$$

The *gasification* process occurs as the char reacts with carbon dioxide and steam to produce carbon monoxide and hydrogen, via the reaction

$$C + H_2O \rightarrow H_2 + CO$$

In essence, a limited amount of oxygen or air is introduced into the reactor to allow some of the organic material to be burned to produce carbon monoxide

and energy, which drives a second reaction that converts further organic material to hydrogen and additional carbon dioxide.

1.3 Fluidized Bed Gasifier

Air is blown through a bed of solid particles at a sufficient velocity to keep these in a state of suspension. The bed is originally externally heated and the feedstock is introduced as soon as a sufficiently high temperature is reached. The fuel particles are introduced at the bottom of the reactor, very quickly mixed with the bed material and almost instantaneously heated up to the bed temperature. As a result of this treatment the fuel is pyrolysed very fast, resulting in a component mix with a relatively large amount of gaseous materials. Further gasification and tar-conversion reactions occur in the gas phase. Most systems are equipped with an internal cyclone in order to minimize char blow-out as much as possible. Ash particles are also carried over the top of the reactor and have to be removed from the gas stream if the gas is used in engine applications.

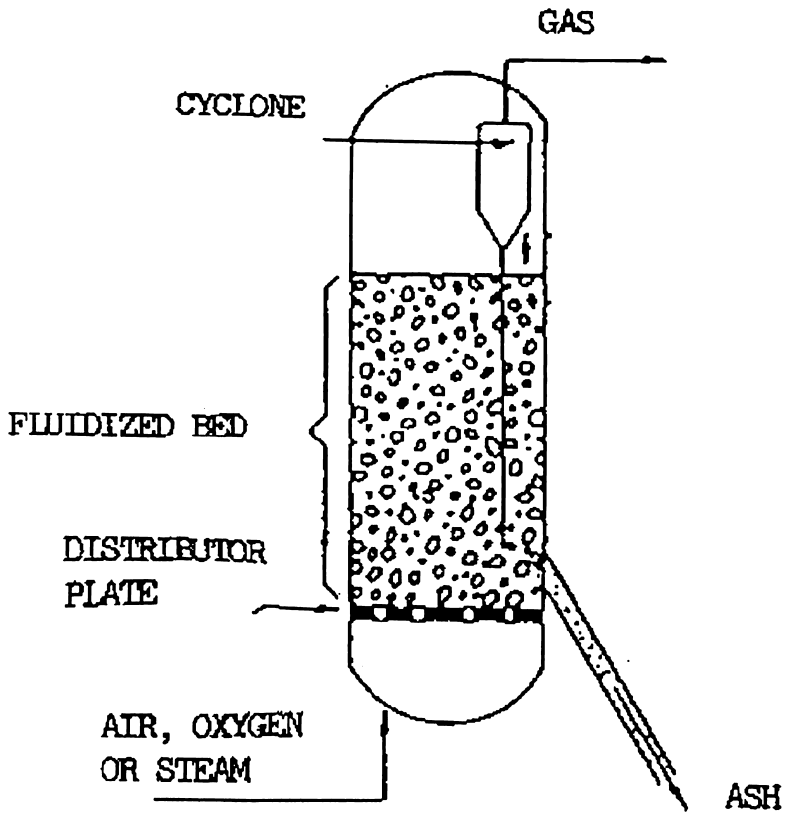

Fig. 1. Schematic diagram of fluidized bed reactor.

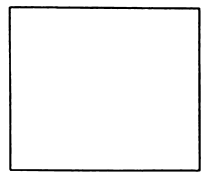

Modeling of the coal gasification process has received significant emphasis over the last two decades. Chejne-Hernandez [1] developed a steady state model for gasification in a fluidized bed. They used a zero-dimensional model for solid phase and one-dimensional model for gas phase approximating the flow type as plug. de-Souza Santos [2,3] developed a comprehensive mathematical model and computer program to use as a tool for engineering design and operation optimization, by predicting the behavior of a real unit during steady-state operation. This model is considered to be complete. Kim et al. [4] proposed a model for coal gasification in an internally circulating fluidized bed based on the bed hydrodynamics and reaction kinetics using shrinking core model for combustion and gasification reactions. Ross et al. [5] focused on a bubbling fluidized bed Gasifier describing the non-isothermal behavior of the gases and heat transfer mechanisms in the bed. Adanez et al. [6] presented a paper with kinetic information of CO_2 gasification process in a fluidized bed.

Understanding of coal and char reaction behavior is essential to the modeling of coal gasification. A number of models have been developed to simulate coal gasification processes in a fluidized bed [7-10]. Most of the models [1-3] for coal gasification reported in literature use the concept of Thiele Modulus to find individual rates of heterogeneous reactions occurring in the coal particles and compute the net production rate by summing these individual rates weighted by respective stoichiometric coefficients. However, Thiele Modulus can be used to compute reaction rate only in a single reaction system. A closer look at the derivation of this expression for heterogeneous rates will tell us that this method is not completely correct.

The purposes of this study are to analyze the application of Thiele Modulus to multiple heterogeneous reactions for evaluating the effective reaction rate, develop a model for gasification reaction in a fluidized bed reactor, and highlight the differences between the two model approaches. An outline of the gasification reaction model is described in the following sections.

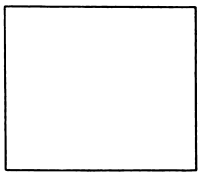

Our goal is to develop an accurate model for heterogeneous reaction rates for gasification of coal in a fluidized bed. In his work [2-4], de Souza Santos has derived rate expressions for heterogeneous reactions involving two distinct phases – solid and gas. The final expression for rate of consumption/production shows the dependency on the barriers imposed by several resistances – Gas film, Ash layer diffusion and Reaction resistance. This expression derived by de Souza Santos considering the species to have participated in a single reaction and to find the net rate of production / consumption, all the rates are summed weighted by the respective stoichiometric coefficients. Many works, reported in literature [1,5-8], on modeling of coal gasification use this result. We instead try to take a different approach to derive the rate expression for multiple-reactions-heterogeneous system and use the net rate in the gasification process in a fluidized bed. When analytical solutions are not feasible, we resort to numerical procedures for the calculating the net rate in a single particle.

This approach will also give us the opportunity to fabricate the model for non-first order multiple reactions system. It could also accommodate any type of particle geometry - plane or cylindrical or spherical. Characterization of the feed and using an appropriate model or combination of models could predict the system to great accuracy. In this thesis, we present this integrated model approach for particle kinetics for multiple reactions and its impact on the temperature profiles and conversion levels.

The developed new approach for heterogeneous reactions rates is used in the model for coal gasification in a fluidized bed.

4.1 Single Reaction – Particle Kinetics

Combustion and Gasification reactions of coal are heterogeneous reactions. They involve two distinct phases: solid and gas. This gives rise to the possibility of mass transfer process affecting the overall production rate. Depending on the rates of reaction, the rate might be controlled or limited by the pace of that mass transfer. Different models have been proposed to in literature [11,12] to describe this process.

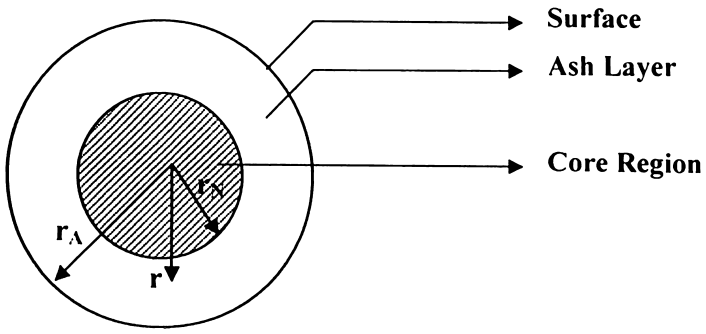

Fig. 2. Shrinking core model for gas – solid particle reactions. [11]

The shrinking core model was chosen for combustion and gasification reactions. It has been observed that this phenomenon was the closest approximation to conditions in a fluidized bed [11]. A near spherical shape of the particle is considered.

$$D_s \frac{1}{r^2}\frac{d}{dr}\left(r^2 \frac{dC_A}{dr}\right) = -R_A \qquad (1)$$

where R_A is the net production of component A. For the present, it is assumed that the rate of consumption of any component (reacting with the solid) due to pure kinetics can be written in the following form:

$$r_A = -kC_A^n \qquad (2)$$

where k is the reaction rate coefficient. This is called the intrinsic reaction rate, as opposed to the effective reaction rate, which is the one calculated after the influence of mass transfer resistances, as deduced below.

In order to transform Eq. (1) in a dimensionless form, the following change of variables is used:

$$x = \frac{r}{r_A} \tag{3}$$

$$y = \frac{C_A}{C_A^{bulk}} \tag{4}$$

Given the treatment for a single reaction and on the basis of each consumed mole of reacting gas component, Eq. (1) can be rewritten as

$$\nabla^2 y = \Phi^2 y'' \tag{5}$$

where Φ is the Thiele Modulus given by Eq.(6).

$$\Phi = r_A \left[\frac{k\left(C_A^{bulk}\right)^{n-1}}{D_s} \right]^{1/2} \tag{6}$$

There is no reaction in the ash layer. Eq. (5) is modified for the ash layer as

$$\nabla^2 y = 0 \tag{7}$$

Solving for the concentration profile inside the coal particle requires three boundary conditions: One at the core centre, one at the core region – ash layer interface and one at the surface of the particle (ash layer – gas film interface).

Boundary Conditions:

1) Core centre:

y should be finite at the centre

2) Core – Ash interface

Flux should be continuous at the interface

$$D_{s,N} \left.\frac{dC_A}{dr}\right|_{r=r_c} = D_{s,A} \left.\frac{dC_A}{dr}\right|_{r=r_c} \tag{8}$$

3) Ash – Gas layer interface

Flux at the surface = rate of mass transfer

$$D_{s,N}\left.\frac{dC_A}{dr}\right|_{r=r_1^-} = \beta_{(i)}\left(C_A^{bulk} - C_A^{surface}\right) \tag{9}$$

The equations (Eq. (5) - (9)) are solved analytically and numerically for coal combustion reaction and the results are discussed.

$$C + \beta O_2 \rightarrow (2\beta - 1)CO_2 + (2 - 2\beta)CO$$

Where β is a measure of relative amounts of CO_2 and CO produced [4]. It is a function of temperature and its value varies between 0.5 and 1.

$$\alpha = \frac{CO}{CO_2} = 2500\exp\left(-\frac{6240}{T}\right) \tag{10}$$

$$\beta = \frac{2+\alpha}{2+2\alpha} \tag{11}$$

Analytical solution for equations (Eq. (5) - (9)) is provided in [2-3,11]. The same system of equations is solved using numerical procedures. The differential equation is discretized first order forward in space. The resulting system of linear equations along with the boundary conditions, presented below, form a tridiagonal matrix system. Gauss Elimination technique was used to solve this set of linear equations.

$$x_i^2 y_{i+1} - \left(x_i^2 + x_{i-1}^2\right) y_i + \left(1 - \Phi^2\delta^2\right) x_{i-1}^2 y_{i-1} = 0 \tag{12}$$

for $2 \le i \le k-1$ (Core)

$$x_i^2 y_{i+1} - \left(x_i^2 + x_{i-1}^2\right) y_i + x_{i-1}^2 y_{i-1} = 0 \tag{13}$$

for $k+1 \le i \le n-1$ (Ash Layer)

Boundary Conditions:

$$y_1 = y_2 \tag{14}$$

$$y_{k+1} - y_k = y_k - y_{k-1} \tag{15}$$

$$(1 + N_1\delta) y_n - y_{n-1} = N_1\delta \tag{16}$$

Results

The effect of factors such as grid size, Sherwood Number, Thiele Modulus and Order of Discretization, on the solution is discussed.

4.1.1 Grid Size

The system of equations developed in section 4.1 is solved for N1 = 10 and Φ = 10

From Fig. 3(a). and Fig. 3(b). , it is observed that the numerical solution gets closer to the analytical solution as the grid size gets finer. This accuracy of the numerical solution is quantified (Table 1) by evaluating the correlation coefficient between analytical and numerical solution for the concentrations.

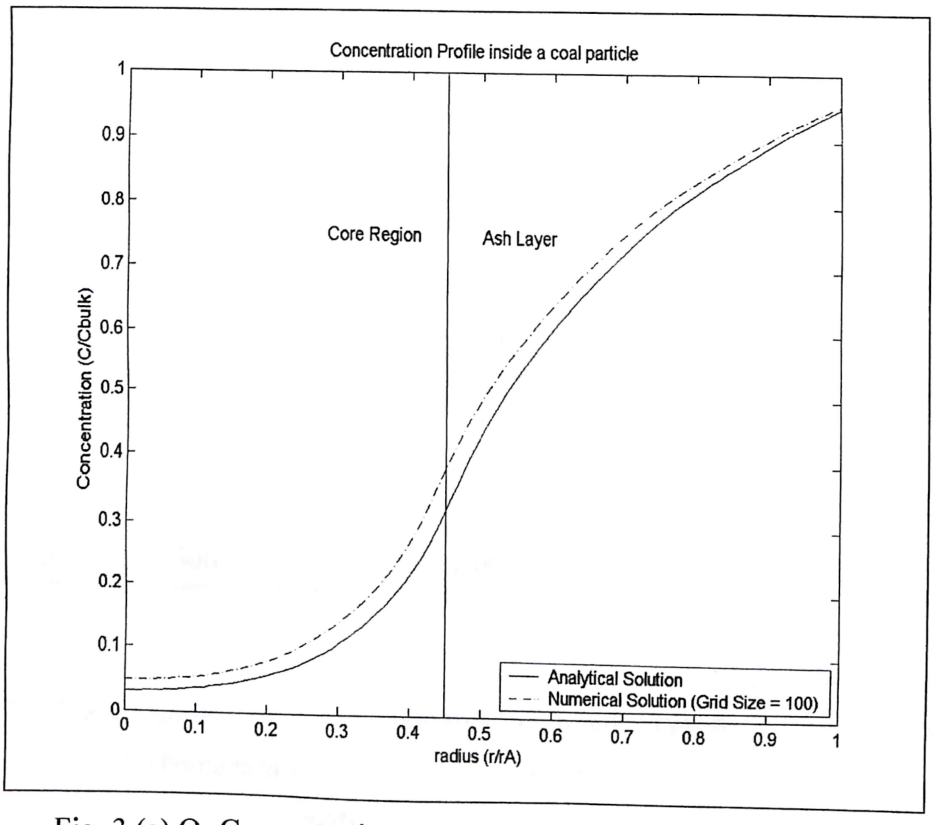

Fig. 3 (a) O_2 Concentration inside a particle: Lower Grid Number

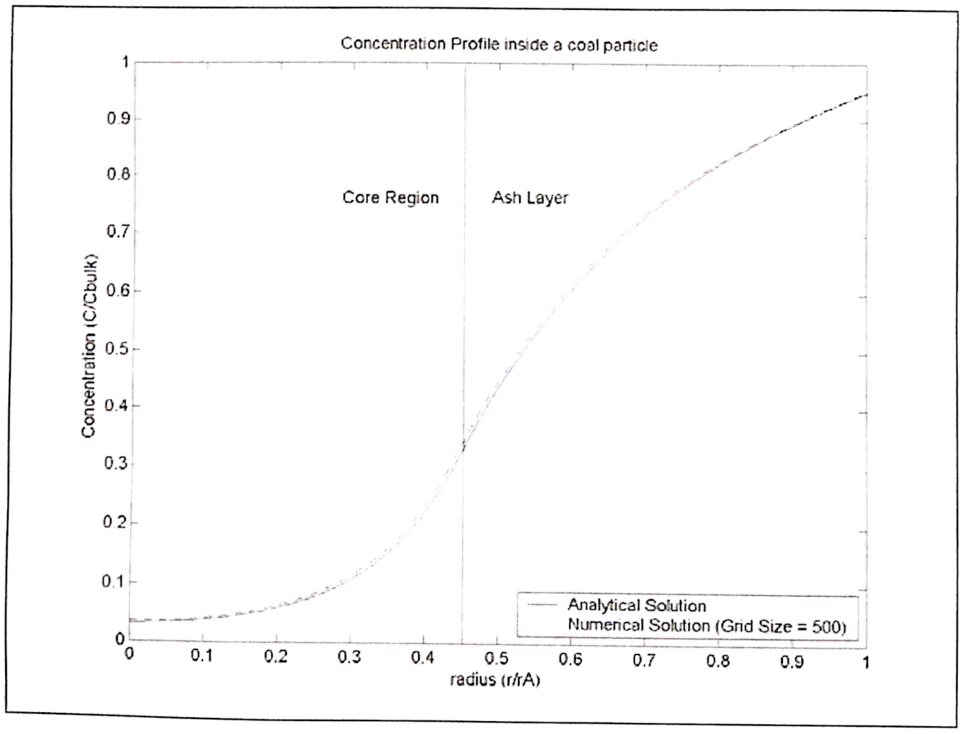

Fig. 3 (b) O_2 Concentration inside a coal particle: Higher Grid Number

Table 1

No.	Grid Size (N)	Correlation Coefficient (r^2)
1	25	0.9912
2	50	0.9966
3	100	0.9990
4	300	0.9999
5	500	1.0000

For grids finer than 500, correlation coefficient was found to be remain at 1. This threshold grid size is remains unaltered when the parameters N1 and Φ are varied. Hence this value is used in computing concentration profiles.

Concentration profiles inside the particle are found. The flux at the boundary is calculated. This gives the net production/consumption of the gaseous components. The boundary conditions, hence, becomes important. To improve accuracy in the solution, the boundary conditions were discretized to higher

orders of accuracy. It was observed that improvement in solution was less than 0.1%. This refinement was minimal and hence first order accurate discretization at the boundary was used.

4.1.2 Sherwood Number

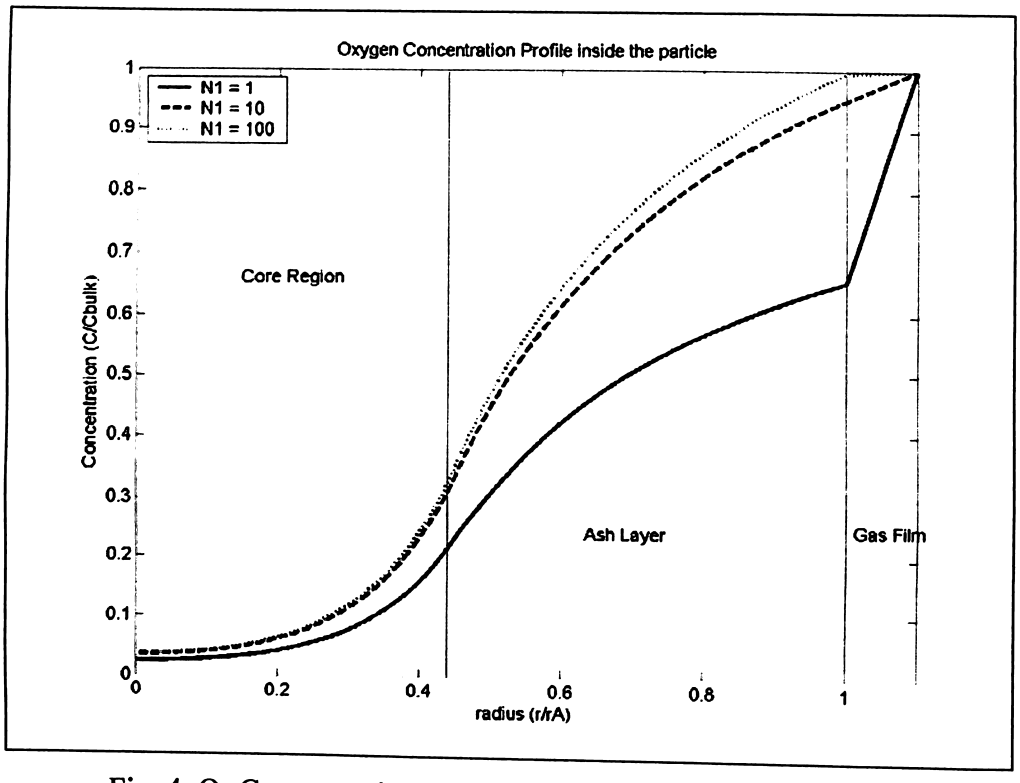

Fig. 4. O_2 Concentration Profile at different Sherwood Number

Table 2

N1	$\Delta C_{film} / \Delta C_{ash}$
1	0.8086
10	0.0809
100	0.0081

From Table 2, it is inferred that higher the values of N1, lower is the ratio of concentration gradient across gas film to that across ash layer. Lower the ratio

of concentration gradient across gas film to that across ash layer, higher is ratio of mass transfer across gas film to that across ash layer. It is observed that this is in agreement with the definition of N1.

$$N1 = Sh\frac{D_G}{D_S} = \frac{hr_A}{D_S} = \frac{h}{\frac{D_S}{r_A}} = \frac{\text{mass transfer across gas film}}{\text{mass transfer across ash layer}} \qquad (17)$$

4.1.3 Thiele Modulus (Φ)

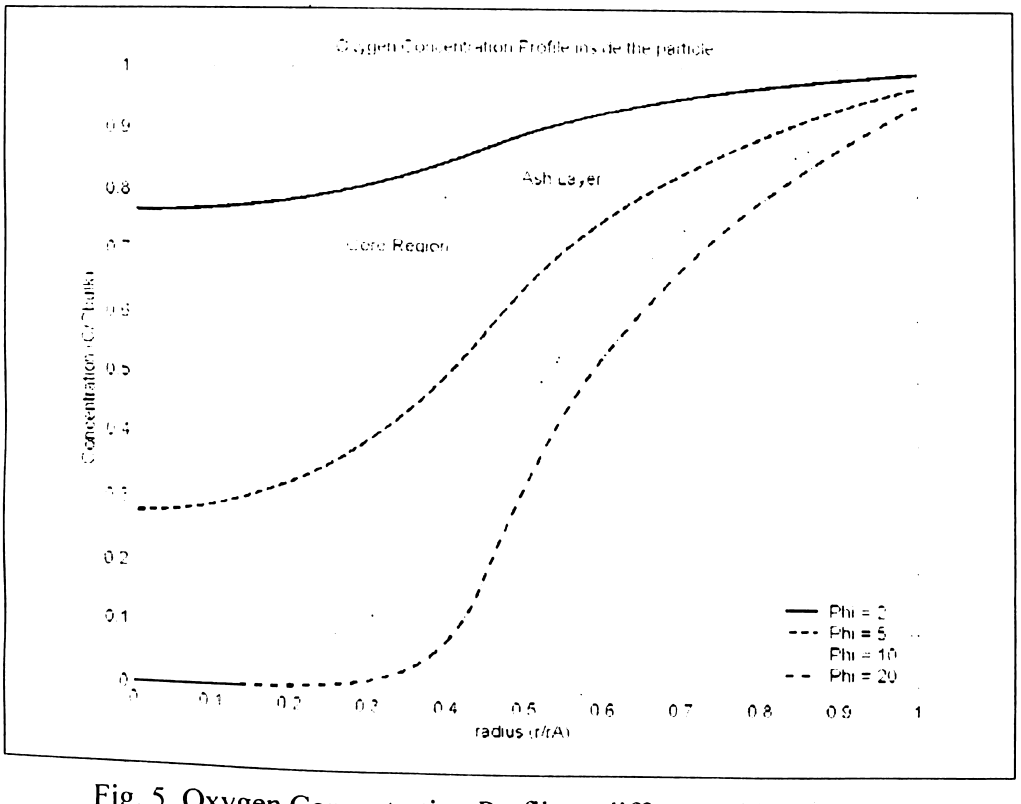

Fig. 5. Oxygen Concentration Profile at different Thiele Modulus

$$\Phi = r_A\left[\frac{k}{D_S}\right]^{1/2} \qquad (18)$$

Thiele Modulus is the ratio of surface reaction rate to the diffusion rate. When the Φ is large, internal diffusion usually limits the overall rate of reaction; when Φ is

small. The surface reaction is usually rate limiting. That is when Φ is small, reaction rate is lower and diffusion is higher and hence the concentration gradient between the particle's centre and its surface is small. And when Φ is high, reaction rate is higher and diffusion is lower and hence the concentration gradient across the particle's centre and its surface is high. This is in agreement with the observation from the above figure.

These factors validate the numerical method for computing gas concentration profile inside a coal particle.

4.2 Multiple Reactions

System of heterogeneous reactions listed in Table 3 is considered.

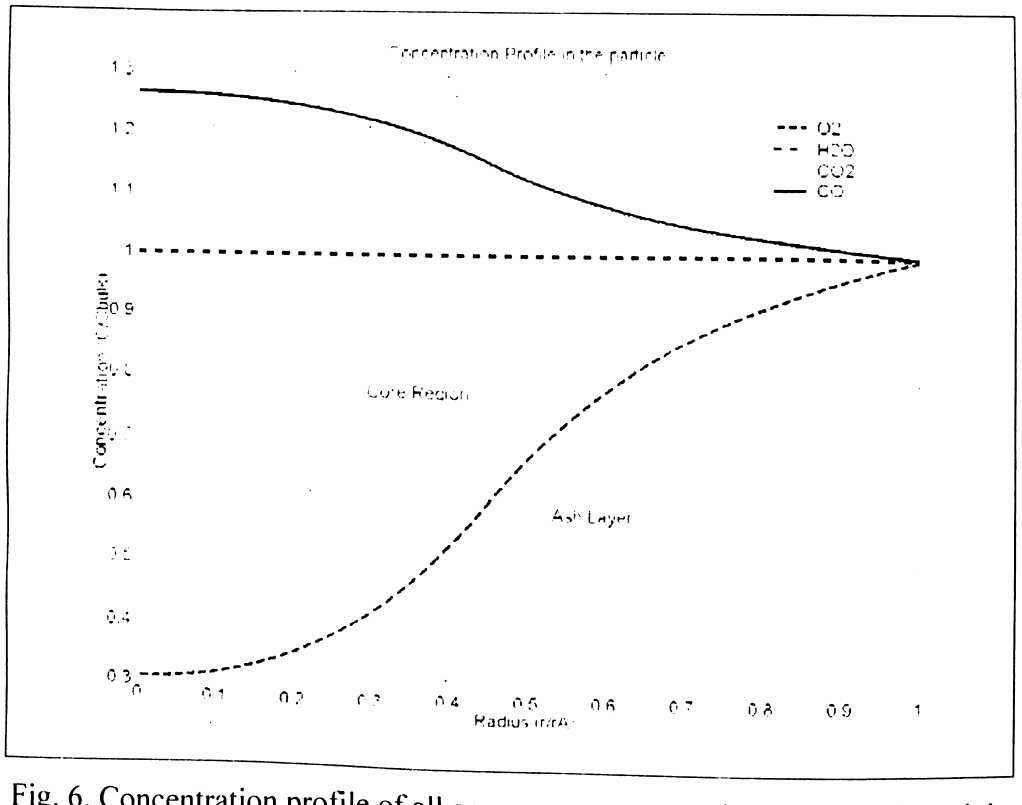

Fig. 6. Concentration profile of all gaseous components inside the coal particle

Following observations are made, from Fig. 6.,

(i) O_2 concentration decreases as it diffuses through the particle from the surface. This is expected due to the net consumption of oxygen from the combustion of coal (R1).

(ii) H2O concentration is almost a constant because of the low rate constant value. The reaction rate is slow. Diffusion dominates and hence a constant profile is observed.

(iii) $$\nabla^2 y_3 = \phi_3^2 y_3 - (2\beta - 1)\lambda_{13}\phi_1^2 y_1 \qquad (19)$$

CO2 is formed from R1 and consumed in R3. But at the temperature at which the reactor is operated, it is observed that the production from R1 dominates consumption from R3 and hence there is a net flux of CO_2 coming out of the particle. The other case where CO_2 consumption in R3 becomes dominant is highlighted in Fig. 7. where the temperature of reactor is increased beyond 1000K. The rate constant of R3 increases at a faster rate with temperature than that of R1 does and hence the R3 becomes dominant. Since the consumption rate (R3) is more than production (R1) rate, CO_2 concentration decreases as it diffuses into the particle.

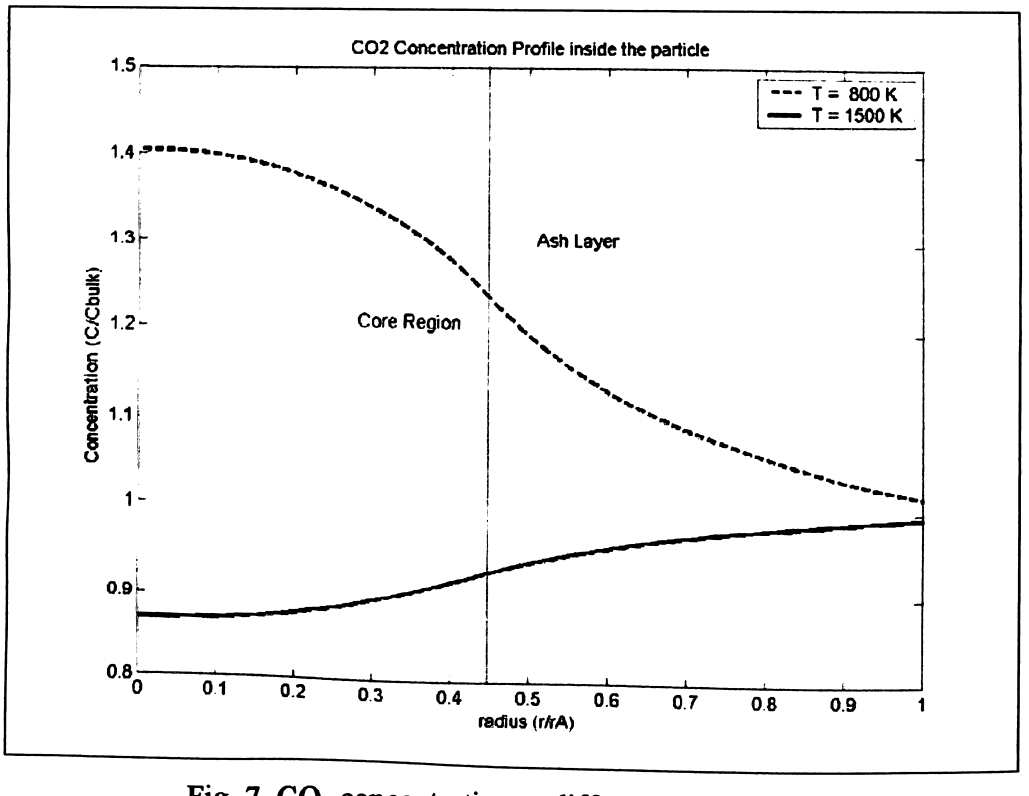

Fig. 7. CO_2 concentration at different temperatures

(iv) $$\nabla^2 y_4 = -\left((2-2\beta)\lambda_{14}\phi_1^2 y_1 + \phi_2^2 \lambda_{24} y_2 + 2\phi_3^2 \lambda_{34} y_3\right) \quad (20)$$

CO is formed from R1, R2 and R3. CO is being produced from all three reactions. Hence the concentration will be increasing inside the particle. And hence, CO will always be diffusing out of the particle.

Thus, the net rates of production/consumption of all the components are calculated by computing the flux at the particle surface from the concentration profiles. This calculation is done at every point along the height of the bed and the results are used in the overall mass balance equations of the corresponding components.

A one-dimensional steady-state mathematical model and a numerical algorithm have been developed to simulate the coal gasification process in a fluidized bed under isothermal conditions. The proposed model is applied to solid particles submerged in a fluidized gas. The solids enter into the reactor at the feed point; the particle size and flowrate is specified at this point. The gas (air and steam) enters through the bottom of the reactor, its inlet composition and flowrates are specified.

A system of six chemical reactions (Table 3) in the solid and gas phase were included.

5.1 Chemical Reactions

Table 3

Reaction	Type	Chemical Reaction	Reference
R1	Solid - Gas	$C+\beta O_2 \rightarrow (2\beta-1)CO_2+(2-2\beta)CO$	[2-3]
R2	Solid - Gas	$C+H_2O \rightarrow CO+H_2$	[1]
R3	Solid - Gas	$C+CO_2 \rightarrow 2CO$	[1]
R4	Gas - Gas	$CO+H_2O \leftrightarrow CO_2+H_2$	[2-3]
R5	Gas - Gas	$2CO+O_2 \leftrightarrow 2CO_2$	[2-3]
R6	Gas - Gas	$2H_2+O_2 \leftrightarrow 2H_2O$	[2-3]

5.2 Model Equations

Before setting equations, we develop a clear list of model assumptions.

1. Steady-state assumption
2. Plug-flow conditions for both gas and solid flows
3. Momentum transfers between the two phases are negligible
4. Inviscid flow for the two phases
5. Flat temperature and concentration profile

The mass balance for the solid and gas phases require that the variation of each component along the axial direction is equivalent to the generation (or consumption) from the heterogeneous reactions.

$$\frac{dF_i^S}{dz} = \left(R_{het,i}\right)\frac{dA_S}{dz} \tag{21}$$

$$\frac{dF_i^G}{dz} = \left(R_{het,i}\right)\frac{dA_S}{dz} + \left(R_{\hom,i}\right)\frac{dV_G}{dz} \tag{22}$$

Where

$$R_{het,i} = M_i \sum_{j=1}^{3} \gamma_{ij} R_j \tag{23}$$

$$R_{\hom,i} = M_i \sum_{j=4}^{6} \gamma_{ij} R_j \tag{24}$$

For CO_2 and CO flowrates,

Method used in literature:

$$\frac{dF_{CO_2}^G}{dz} = \left(\left(2\beta - 1\right)R_1 - R_3\right)M_{CO_2}\frac{dA_S}{dz} \tag{25}$$

$$\frac{dF_{CO}^G}{dz} = \left(\left(2 - 2\beta\right)R_1 + R_2 + R_3\right)M_{CO}\frac{dA_S}{dz} \tag{26}$$

Where

$$R_i = -D_S\left.\frac{dC_i}{dr}\right|_{r=r_i^-} = -D_S\left.\frac{C_i}{r_i}\frac{dy_i}{dx}\right|_{x=1^-} = \frac{2}{d_p}\frac{C_i}{R_{mtl,i}} \tag{27}$$

$$R_{mtl,i} = \frac{1}{ShD_{Gi}} + \frac{1-a}{aD_S} + \frac{1}{aD_S\left(a\Phi_i\coth\left(a\Phi_i\right) - 1\right)} \tag{28}$$

dy_i/dx in Eq. (27) is found by analytical solution of Eq. (29-34) .

For $0 < x < a$

$$\nabla^2 y_1 = \phi_1^2 y_1 \tag{29}$$

$$\nabla^2 y_2 = \phi_2^2 y_2 \tag{30}$$

$$\nabla^2 y_3 = \phi_3^2 y_3 \tag{31}$$

For $a < x < 1$

$$\nabla^2 y_1 = 0 \tag{32}$$

$$\nabla^2 y_2 = 0 \tag{33}$$

$$\nabla^2 y_3 = 0 \tag{34}$$

Method used in this work:

$$\frac{dF_{CO_2}^G}{dz} = (CO_2 Rate) M_{CO_2} \frac{dA_S}{dz} \tag{35}$$

$$\frac{dF_{CO}^G}{dz} = (CO Rate) M_{CO} \frac{dA_S}{dz} \tag{36}$$

Where

$$CO_2 Rate = -D_S \left.\frac{dC_{CO_2}}{dr}\right|_{r=r_1^-} = -D_S \frac{C_{CO_2}}{r_A} \left.\frac{dy_3}{dx}\right|_{x=1^-} = -D_S \frac{C_{CO_2}}{r_A} \frac{y_3'' - y_3^{n-1}}{\delta} \tag{37}$$

$$CO Rate = -D_S \left.\frac{dC_{CO}}{dr}\right|_{r=r_1^-} = -D_S \frac{C_{CO}}{r_A} \left.\frac{dy_4}{dx}\right|_{x=1^-} = -D_S \frac{C_{CO}}{r_A} \frac{y_4'' - y_4^{n-1}}{\delta} \tag{38}$$

Where y3 and y4 are found by numerical solutions of Eq. (39-46).

For $0 < x < a$

$$\nabla^2 y_1 = \beta \phi_1^2 y_1 \tag{39}$$

$$\nabla^2 y_2 = \phi_2^2 y_2 \tag{40}$$

$$\nabla^2 y_3 = \phi_3^2 y_3 - (2\beta - 1) \lambda_{13} \phi_1^2 y_1 \tag{41}$$

$$\nabla^2 y_4 = -\left((2 - 2\beta) \lambda_{14} \phi_1^2 y_1 + \phi_2^2 \lambda_{24} y_2 + 2\phi_3^2 \lambda_{34} y_3\right) \tag{42}$$

For $a < x < 1$

$$\nabla^2 y_1 = 0 \tag{43}$$

$$\nabla^2 y_2 = 0 \tag{44}$$

$$\nabla^2 y_3 = 0 \tag{45}$$

$$\nabla^2 y_4 = 0 \tag{46}$$

where $y_i = \frac{C_i}{C_i^{bulk}}$ and $\lambda_{ij} = \frac{C_i^{bulk}}{C_j^{bulk}}$

Table 4

i	Component
1	O_2
2	H_2O
3	CO_2
4	CO

In the method reported in literature, it was assumed that each heterogeneous reaction occurs individually inside a coal particle. In this work, a more accurate procedure is used relaxing this assumption. It takes into all reactions occurring simultaneously inside the coal particle and the net rate of production is found.

It can be observed that y_1 and y_2 are independent of the other two variables (y3 and y4). Analytical solutions can be obtained for y_1 and y_2. However, y_3 and y_4 are dependant on other variables. Numerical solution scheme described in chapter 4 is used to compute y_3 and y_4.

5.3 Boundary Conditions

The boundary conditions used in the program, for the mass balance equations Eqs. (21, 22, 35, 36) corresponds to the feed conditions of the bed.

Table 5

Inlet Flowrate / Temperature	Value
Coal (kg/hr)	8
Air (kg/hr)	21.9
Steam (kg/hr)	4.62
Gas Temperature (K)	700
Reactor Temperature (K)	800

5.4 Auxiliary Equations

Some of the equations necessary to complete the set of model equations are presented in this section.

5.4.1 Area of Particles and Volume occupied by solid phase

The ratio of particle area per vertical length of the bed can be computed by

$$\frac{dA_S}{dz} = S(1-\varepsilon)\frac{A_p}{V_p} f^{"} = S(1-\varepsilon)\frac{6}{d_p} f^{"} \qquad (47)$$

where the parameter $f^{"}$ represents the volume fraction of carbonaceous solid in the solid phase.

5.4.2 Diffusivities

5.4.2.1 Gas – Gas Diffusion

As a first approximation, we have assumed that all gases diffuse at the same rate into the coal particle. This is possible because the average molecular mass of the commonly present gases in the gasifier or even furnaces processing carbonaceous solids do not change too much from case to case. In this way, the following correlation [13] is used to compute average diffusivities of these gases.

$$D_{Gi} = 8.667 \times 10^{-5} \frac{T^{1.75}}{P} \qquad (48)$$

5.4.2.2 Gas – Solid Diffusion

Besides the gas-gas diffusion, additional resistances occur when gases diffuse through gas mixture confined in the pores of a solid structure. The combined resistances lead to the concept of effective diffusion coefficient. Many correlations have been proposed to estimate the effective diffusivities through porous solids. According to [14], the effective diffusivity of a gas through a solid is directly proportional to its porosity and inversely to its tortuosity.

$$D_{eff} = \frac{D_{Gi}}{\gamma}\zeta \qquad (49)$$

Where the tortuosity is approximated by

$$\gamma = \frac{1}{\zeta} \tag{50}$$

In this work, it is assumed that the diffusivity in ash layer and diffusivity in core region are same.

$$D_{S,N} = D_{S,A} \tag{51}$$

5.5 Core Dimensions

The dimensions of core are calculated from the fractional conversion of the reacting solid.

$$a = \frac{r}{r_A} = (1-f)^{1/3} \tag{52}$$

where f is the fractional conversion of coal which can be calculated from the flowrate.

$$f = 1 - \frac{F_C}{F_C^0} \tag{53}$$

5.6 Heat and Mass Transfer Coefficients

The coefficients of heat and mass transfer are calculated from Nusselt and Sherwood Numbers.

Sherwood and Nusselt numbers, as the corresponding parameters for mass and heat transfer, are defined by

$$Sh = \frac{\beta_G d_P}{D_G} \tag{54}$$

$$Nu = \frac{\alpha_G d_P}{\lambda_G} \tag{55}$$

Several correlations [15,16] have been reported in literature for different situations. For the present case, correlation proposed by Steinberger RL and Treybal RE [16] is used.

$$Sh = 2 + 1.1 \times \mathrm{Re}^{1/2} Sc^{1/3} \tag{56}$$

$$Nu = 0.4 \left(\frac{\mathrm{Re}}{\varepsilon} \right)^{2/3} \mathrm{Pr}^{1/3} \tag{57}$$

In these empirical and semi empirical correlations, it is assumed that there is no or small interactions between mass and heat transfers.

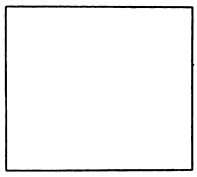

6.1 Choosing Solver

The model includes a total of 9 differential equations with non-constant and non-linear coefficients. As mentioned earlier, the transport coefficients, physical properties, reaction rates are calculated at each point of the bed as functions of composition and temperature. Thus, the model deals with a non-linear and stiff set of equations. Stiffness occurs when there are two or more very different scales of an independent variable, which intern affects the dependant variable. This set of stiff equations is solved in MATLAB 6.5 using ode15s solver. Ode15s [17] is a multi-step solver that uses Numerical Differentiation Formulas (NDFs). Optionally, it uses the backward differentiation formulas (BDFs, also known as Gear's method). For the same time span of integration, it is observed that ode15s takes much less time than what ode45 does.

Table 6

Solver	Time Taken (s)
Ode45	250
Ode23s	2.5
Ode15s	1

All calculations presented in this work were done on HCL desktop, model HCM780M of configuration 3.00 GHz Pentium 4 processor and 1GB RAM. The convergence criterion for flowrate and temperature variables was that the relative tolerance is less than 1e-3.

$$\left|\frac{F_{i+1}-F_i}{F_i}\right| < 10^{-3} \qquad (58)$$

6.2 Discretization of differential equations

The equations () are obtained from first order discretization of Eq.() for CO_2 and CO along with the boundary conditions. X = 0 to 1 is discretized into n grids.

$$x_i = \frac{i-1}{n-1} \text{ for } 1 \le i \le n \tag{59}$$

$$k = \frac{r}{r_1}(n-1) \text{ where k marks the core-ash layer interface.} \tag{60}$$

CO2:

$$x_i^2 y_3^{i+1} - \left(x_i^2 + x_{i-1}^2\right) y_3^{i} + \left(1 - \Phi_3^2 \delta^2\right) x_{i-1}^2 y_3^{i-1} = -\left(2\beta - 1\right) \lambda_{13} \Phi_1^2 \delta^2 x_{i-1}^2 y_1^{i-1} \tag{61}$$

for $2 \le i \le k-1$ (Core)

$$x_i^2 y_3^{i+1} - \left(x_i^2 + x_{i-1}^2\right) y_3^{i} + x_{i-1}^2 y_3^{i-1} = 0 \tag{62}$$

for $k+1 \le i \le n-1$ (Ash Layer)

Boundary Conditions:

$$y_3^1 = y_3^2 \tag{63}$$

$$y_3^{k+1} - y_3^k = y_3^k - y_3^{k-1} \tag{64}$$

$$\left(1 + N_1 \delta\right) y_3'' - y_3^{n-1} = N_1 \delta \tag{65}$$

CO:

$$x_i^2 y_4^{i+1} - \left(x_i^2 + x_{i-1}^2\right) y_4^{i} + x_{i-1}^2 y_4^{i-1} = -\delta^2 x_{i-1}^2 \left(\left(2 - 2\beta\right) \lambda_{14} \Phi_1^2 y_1^{i-1} + \lambda_{24} \Phi_2^2 y_2^{i-1} + \lambda_{34} \Phi_3^2 y_3^{i-1}\right) \tag{66}$$

for $2 \le i \le k-1$ (Core)

$$x_i^2 y_4^{i+1} - \left(x_i^2 + x_{i-1}^2\right) y_4^{i} + x_{i-1}^2 y_4^{i-1} = 0 \tag{67}$$

for $k+1 \le i \le n-1$ (Ash Layer)

Boundary Conditions:

$$y_4^1 = y_4^2 \tag{68}$$

$$y_4^{k+1} - y_4^k = y_4^k - y_4^{k-1} \tag{69}$$

$$\left(1 + N_1 \delta\right) y_4'' - y_4^{n-1} = N_1 \delta \tag{70}$$

This system of equations forms a tridiagonal matrix system. It is solved using Gauss Elimination method.

6.3 Basic Description of the Algorithm

The program for the proposed model was programmed in MATLAB 6.5 using ode15s solver for integrating along the bed and user-defined function dydx at each step for calculating CO_2 and CO concentration profile inside the particle and their production rates from the heterogeneous reactions.

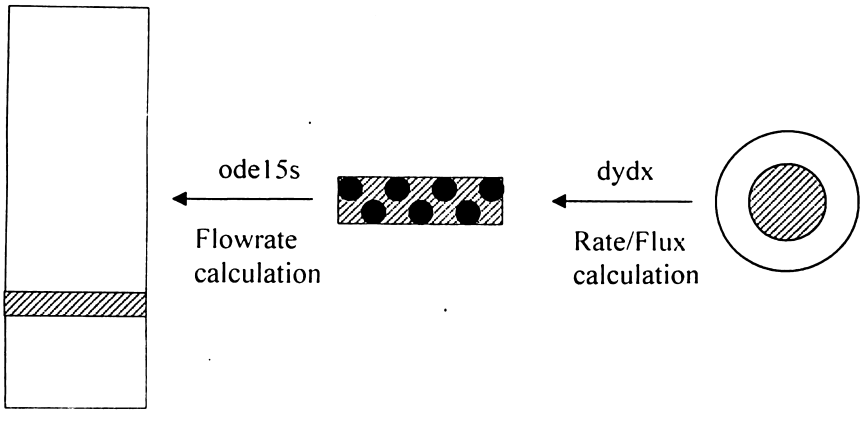

Fig. 8. Program Diagram

The flowrates of all components are evaluated at each point of the bed by integrating set of the mass balance equations derived in Chapter 5 (first order ordinary differential equations) using ode15s solver in MATLAB 6.5.

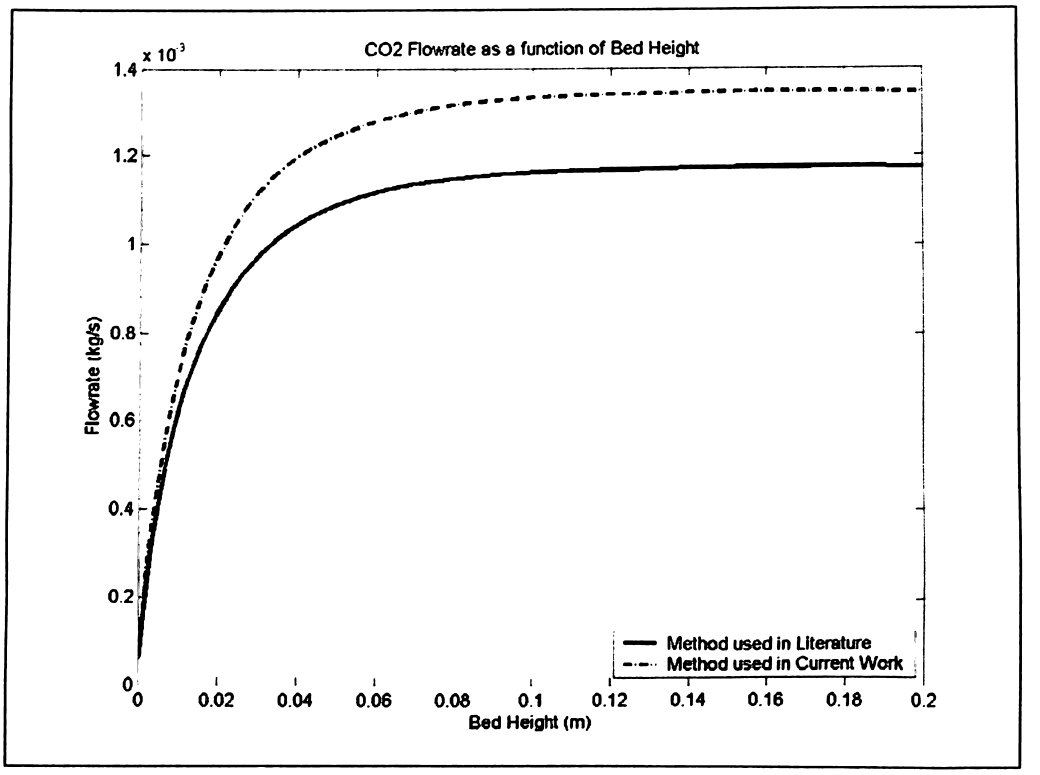

Fig. 9. CO_2 flowrate: Comparison of the two methods

From Fig. 9., it can be observed that CO_2 flowrates computed using the two methods differ. Flowrates computed using the method proposed in this work are higher than those computed using method used in literature. The same is observed in the case of CO (Fig. 10.)

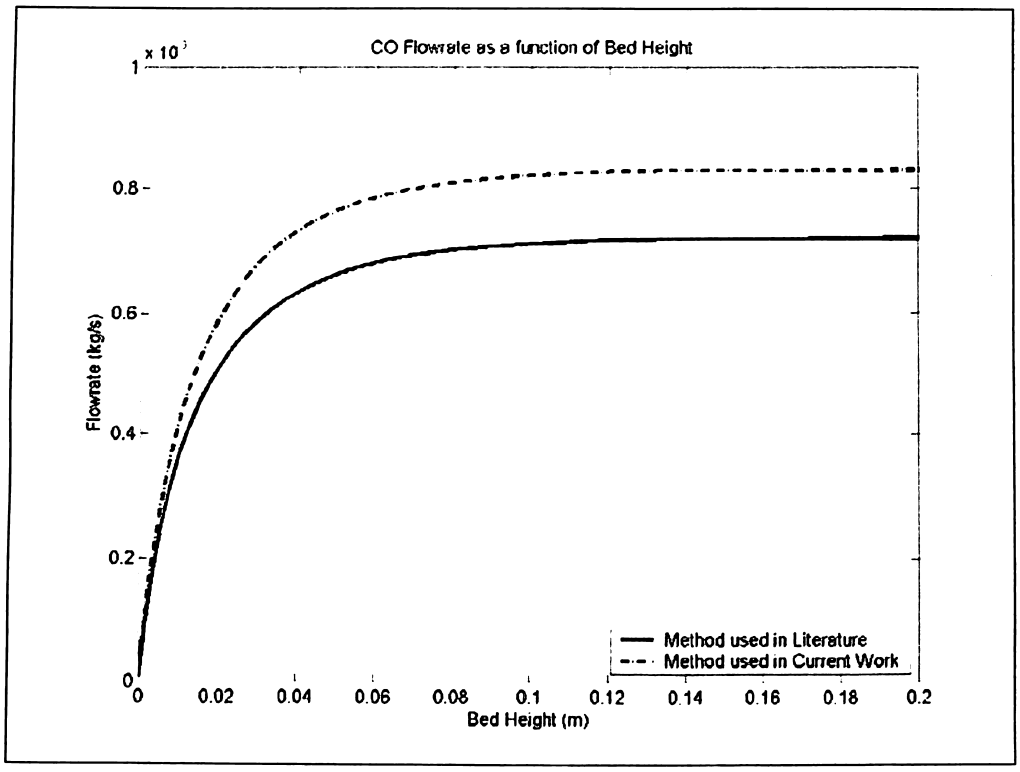

Fig. 10. CO flowrate: Comparison of the two methods

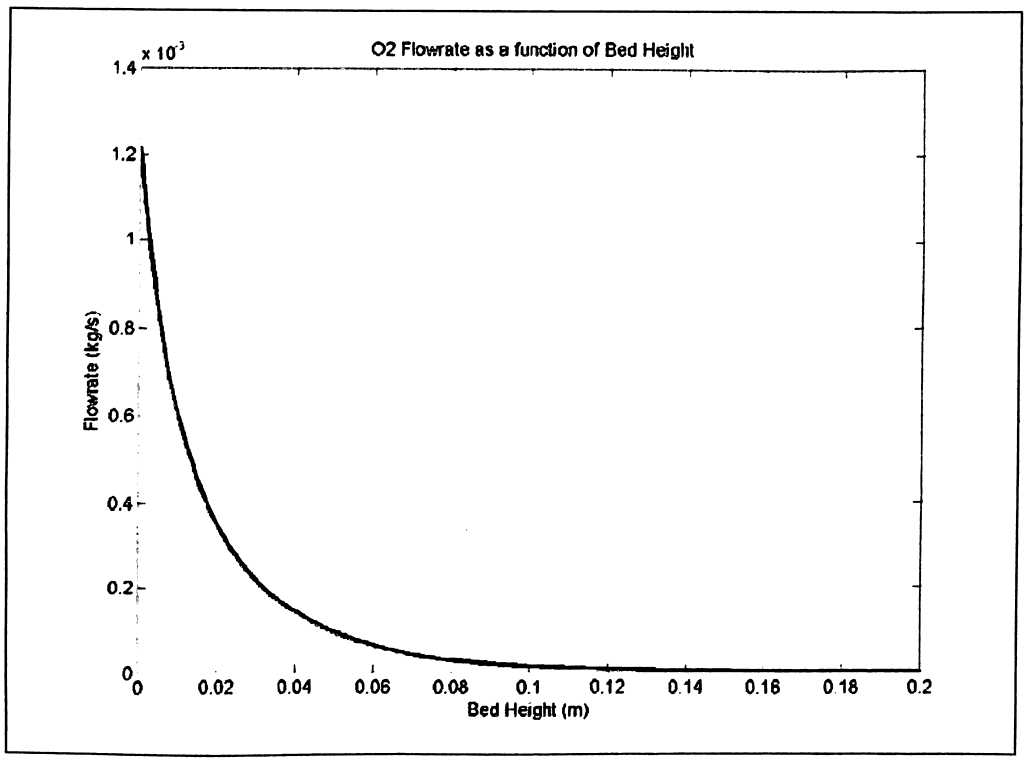

Fig. 11. O_2 flowrate along the bed height

From the kinetic parameters. it can be seen that the combustion process is fast. Hence oxygen is consumed within a few centimeters from the inlet point of gases. This is shown in Fig. 11.

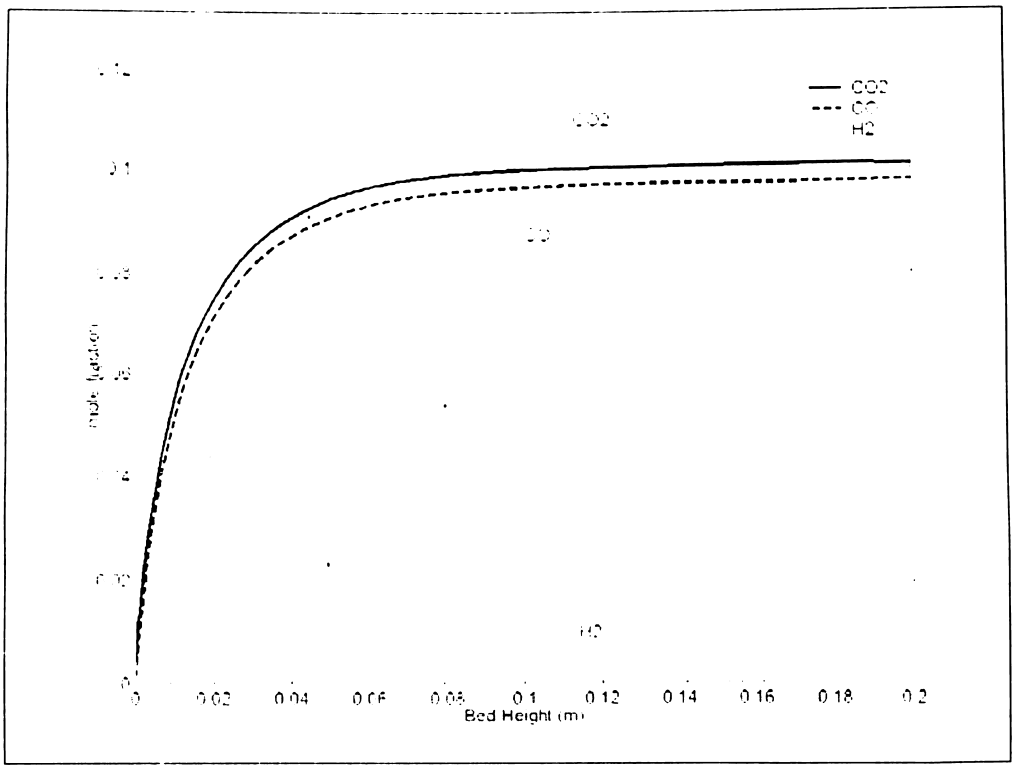

Fig. 12. Molar composition as a function of bed height.

The mole fraction of hydrogen in the gas phase is very low (Fig.12.) because of low rate constant value of steam gasification, reaction from which hydrogen is produced.

Effect of Temperature:

From Fig. 13(a). and Fig. 13(b)., it was observed that the gas phase temperature does not have much effect on the overall production rate of CO_2 and CO where as solid phase temperature seem to have a strong influence. The heterogeneous reactions in solid phase and homogeneous reactions in gas phase, contribute to the overall production rates of CO_2 and CO. The magnitude of available surface area per unit volume, at any section of the bed, is much higher than the magnitude of volume. Hence heterogeneous reactions becomes the

dominant term in the mass balance equations. Hence the effect of solid phase temperature on net production rates of gases is observed to be stronger.

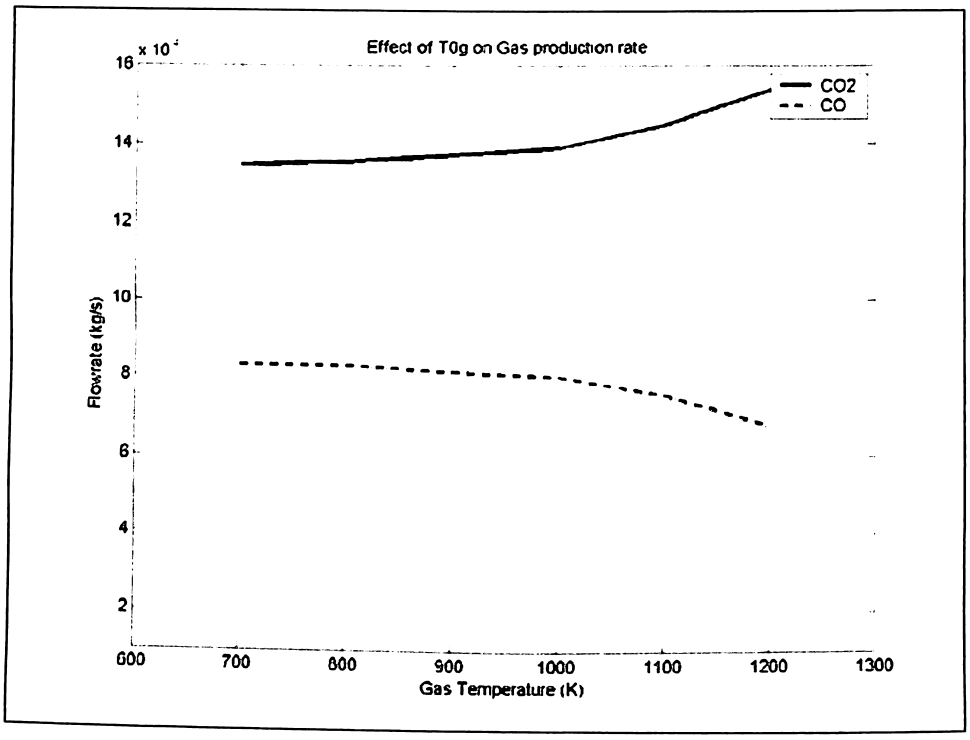

Fig. 13(a). Effect of T_G on CO_2 and CO production rates

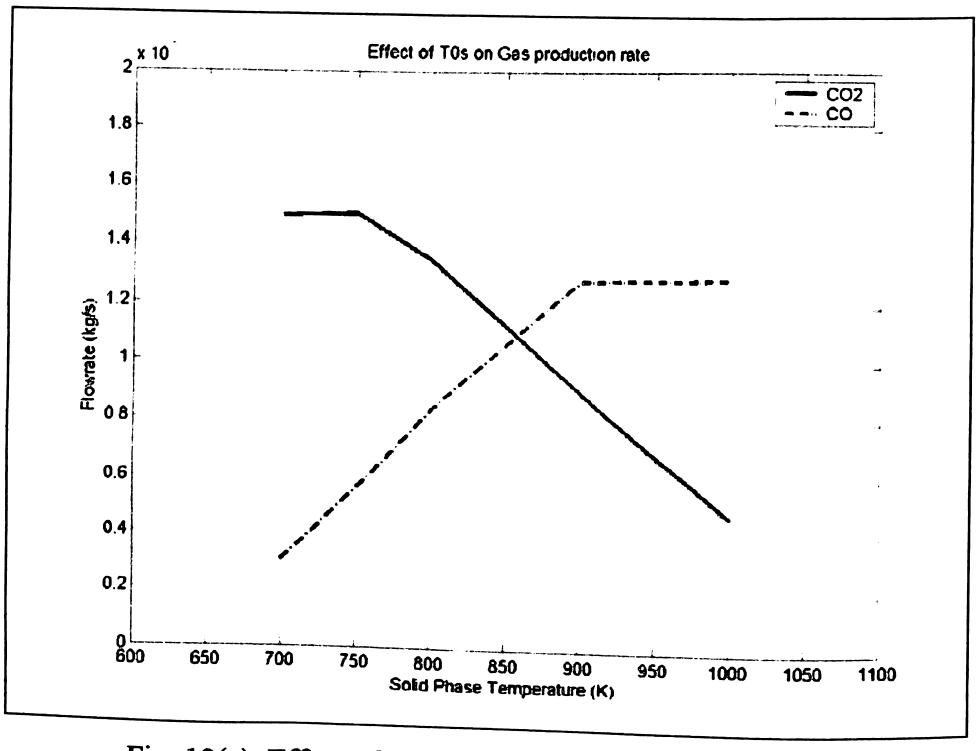

Fig. 13(a). Effect of T_S on CO_2 and CO production rates

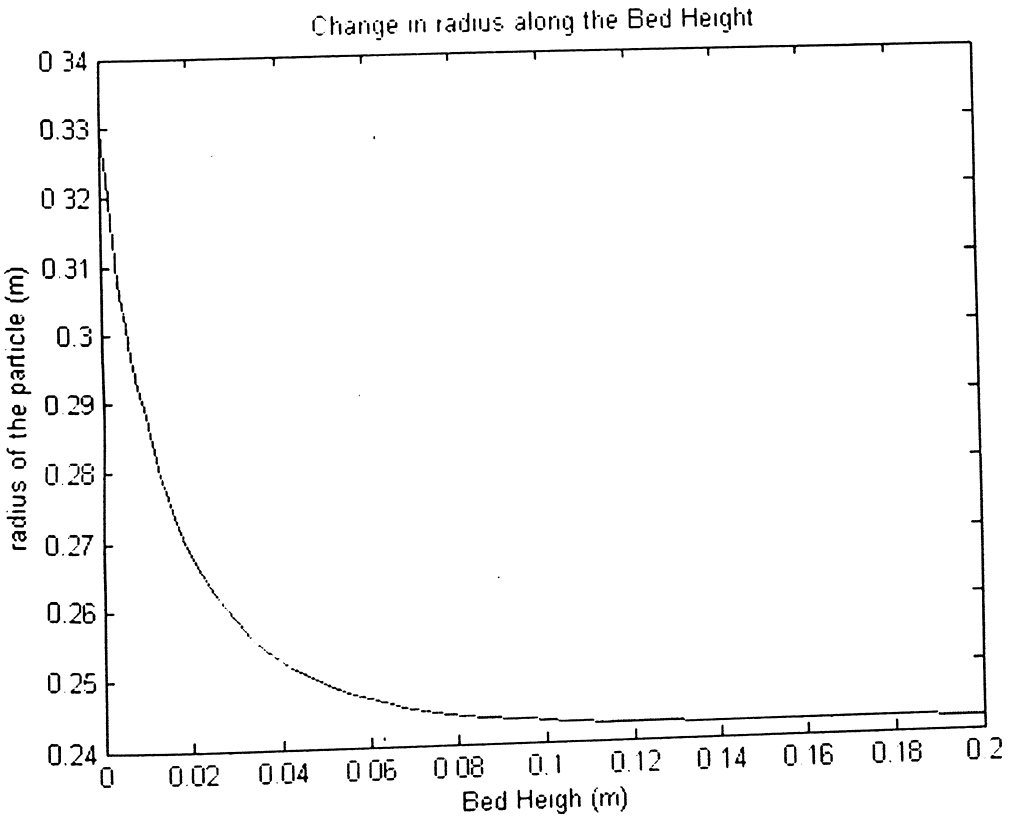

In the above figure the radius of the particle is decreasing along the bed height as the conversion along the bed height is increasing

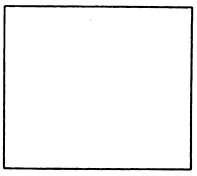

A new model for solid-gas reaction rates has been proposed. Numerical method developed to compute the heterogeneous reaction rates is discussed. The developed model and the numerical algorithm were tested by studying the effect of various parameters such as Sherwood Number, Thiele Modulus and Grid Size on the solution. After validation of the proposed model for solid-gas reactions, Coal gasification process was chosen to apply the new model for computing reaction rates. Results have been presented for the system considered: combustion and gasification of coal.

A one-dimensional steady state mathematical model and a numerical algorithm have been developed to simulate the coal gasification process in fluidized bed. The model incorporates two phases, the solid and the gas. The new model described in the previous section has been used for computing concentration profiles of gases from a system of heterogeneous reactions and their net production/consumption inside a coal particle. These results were used in model equations of the fluidized bed to compute the flowrates as a function of bed height. The model can predict mass flow rates of components in both the phases.

In the present work, isothermal conditions were assumed. Temperature changes along the bed can be included from energy balance. Coal characteristics can be included in the model to improve the predictability of the model. Drying and volatilization of the coal particles can be included in the model.

Numerical procedure developed in this work can be integrated into mathematical models for other kinds of reactors, moving bed and fixed bed. This numerical procedure developed for computing reaction rates in coal gasification process can be extended to other heterogeneous systems involving multiple reactions.

NOMENCLATURE

Symbol	Description	Units
a	Ratio of core radius to outer radius	-
Ar	Cross Sectional Area of the bed	m^2
A_S	Solid Surface area available for heterogeneous reaction	m^2
C_i	Heat Capacity of component i	$J/mol.K$
dH^0	Enthalpy of Reaction	J/mol
d_p	Diameter of particle	m
D_i	Gas Diffusivity in medium i	m^2/s
F_j^i	Flowrate of Component j in phase i	kg/s
k	Reaction Rate Constant	$1/s$
M_i	Molecular Weight of component i	kg/mol
Nu	Nusselt Number	-
Pr	Prandtl Number	-
r_A	Radius of particle	m
Re	Reynolds Number	-
R_i	Rate of reaction i	$mol/m^2.s$
$R_{c,i}$	Heat transfer due to convection	$J/m^2.s$
$R_{Q,i}$	Heat generated due to heat of reaction in phase i	$J/m^2.s$
T_i	Temperature of phase i	K
U_i	Superficial Velocity of Phase i	m/s
Greek Letters		
α	Combustion Kinetic Coefficient	-
β	Combustion Kinetic Coefficient	-
ε	Void Fraction	-
λ_{ij}	Ratio of bulk concentrations of component I to j	-
μ	Viscosity	Pa/s

Φ_i	Thiele Modulus of reaction i	-
ρ_{app}	The weight per unit volume of activated carbon.	kg/m^3
ρ_{real}	The density of the skeleton of a carbon granule.	kg/m^3
γ_{ij}	Stoichiometric coefficient of component I in reaction j	-

Subscripts		
G	Gas Phase	-
P	Particle	-
S	Solid Phase (Ash Layer + Core Region)	-

[1] Chejne F, Hernandez JP. Fuel 2002;81:1687.

[2] de Souza-Santos ML. Fuel 1989;68:1507.

[3] de Souza-Santos ML. Fuel 1994;73:1459.

[4] Kim YJ, Lee JM, Kim SD. Fuel 2000;79:69.

[5] Ross DP, Yan HM, Zhong Z, Zhang DK. Fuel 2005;84:1469.

[6] Adanez J, Miranda JL, Ma. Gavilan J. Fuel 1983;64:802.

[7] Hamel S, Krumm W. Powder Technology 2001;120:105.

[8] Yan HM, Heidenreich C, Zhang DK. Fuel 1999;78:1027.

[9] Everson R, Neomagus H, Kaitano R. Fuel 2005;84:1136.

[10] Manovic V, Komatina M, Oka S. Fuel 2008;87:905.

[11] de Souza-Santos ML. Solid Fuels Combustion and Gasification. Florida: CRC Press, 2004.

[12] Fogler HS. Elements of Chemical Reaction Engineering. 3rd Edn. New Delhi: Prentice Hall, 2002.

[13] Field MA, Gill DW, Morgan BB, Hawksley PGW. Brit. Coal Utiliz. Res. Assc. Mon. Bull. 1967;31:285.

[14] Walker PL, Ruskino F, Austin LG. Gas Reactions of Carbon. In: Advances in Catalysis, Vol XI. New York: Academic Press, 1959.

[15] Treybal RE. Mass Transfer Operations. 2nd Edn. New York: McGraw-Hill, 1968

[16] Steinberger RL, Treybal RE. AIChE J. 1960;6:227

[17] Shampine LF, Reichelt MW. SIAM Journal on Scientific Computing 1997;18:1.

A. MATLAB Program to solve the model equations of coal gasification process in a fluidized bed under isothermal conditions

1) Main Program

```
% 16th April, 2009
% Modeling of Coal Gasification in a fluidized bed reactor
% under isothermal conditions
% by S Phani Kiran

% System:
% C + b O2 --> (2b - 1) CO2 + (2 - 2b) CO
% C + H2O --> CO + H2
% C + CO2 --> 2CO
% CO + H2O <--> CO2 + H2O
% 2 CO + O2 ---> 2 CO2
% 2 H2 + O2 ---> 2 H2O
%
% ---------------------------------------
global dp rA F0 T0 R Ar M Fint As0
global N1 Cin Dg Ds ug us Sh htc Cpg iu
global dH0 To Phi beta SigCp
global T0s T0g F0s F0g Ms Mg P
global rhoapp rhoreal rhobulk eps
% ------------ Constants ------------------
R = 8.314; % Universal Gas Constant (J/mol-K)
% Molecular Weight (kg/mol)
Ms = [12]/1000;
Mg = [32 18 44 28 2 28]/1000;

% ----------- System Dimensions -----------
dp = 0.00062; % Particle Diameter(m)
rA = dp/2;
H = 0.2; % Height of the bed (m)
Dr = 0.22; % Diameter of reactor (m)
Ar = pi/4*Dr^2; % Area (m2)
As0 = Ar;

% --------- Feedrate ---------------------
% Feedrate of C, O2, H20, CO2, CO and H2 resp. (kg/s)
F0s = [8]/3600;
F0g = [0.2*21.9 4.6 0.01*21.9 0.001*21.9 0]/3600;
Fint = 0.79*21.9/3600; % N2 flowrate
T0g = 693; % Inlet Temp of Gases (K)
T0s = 798; % Inlet Temp of Solids (K)

% ---------------- Parameters in the Model------------
alpha = 2500*exp(-6240/T0s); % CO/CO2 ratio in Combustion
Reaction
beta = (2+alpha)/(2+2*alpha); % O2/C consumption

% ---------------- Feed Conditions ------------------
P = 101600; % Reactor Pressure (Pa)
```

```
% Coal Properties:
rhobulk = 980; % Bulk Denisty (kg/m3)
rhoapp = 2000; % Apparent Density (kg/m3)
rhoreal = 2250; % Real Density (kg/m3)
eps = 1 - rhobulk/rhoapp; % Void Fraction
por = 0.3; % Ash porosity
Dg = 1.5e-5*(T0g/298)^1.5*por^1.41; % Diffusivity of gas (m2/s)
Ds = Dg*por^2;

% ---------------- Flow Properties ------------------
Mav = (sum(F0g(1:5).*Mg(1:5)) + Fint*Mg(6))/(sum(F0g(1:5))+Fint);
% Weighted Avg Mol. Wt
rhog = P*Mav/(R*T0g); % Density of Gas (kg/m3)
ug = (sum(F0g(1:5))+Fint)/(Ar*rhog); % Superficial Velocity of
Gas (m/s)
us = F0s/(Ar*rhobulk); % Superficial Velocity of Solid (m/s)
ug0 = ug;
Cin = rhobulk/Ms(1); % Carbon Feed Molar Concentration used in
rate constants (mol/m3)
Mug = 2.3e-6; % Pa.s of Air
Re = dp*ug*rhog/Mug; % Reynolds Number
Sc = Mug/(rhog*Dg); % Schimdts Number
Sh = 2.0 + 1.1*Re^0.5*Sc^(1/3); % Chilton-Colburn Analogy
N1 = Sh*Dg/Ds;

% -------------------- Main ---------------------
IniCond = [F0s F0g F0g(3) F0g(4) As0]; % Initial Conditions
[z,F] = ode15s(@ModelEqns,[0 H],IniCond);

c = F(:,1);
o2 = F(:,2);
h2o = F(:,3);
aco2 = F(:,4);
nco2 = F(:,7);
aco = F(:,5);
nco = F(:,8);
h2 = F(:,6);
As0 = F(:,9);

r = rA*power((c/F0s),(1/3));

Xc = 1 - (r/rA).^3;
Xo2 = 1 - o2/F0g(1);

mo2 = o2./(Ar*ug0*Mg(1));
mh2o = h2o./(Ar*ug0*Mg(2));
mco2 = nco2./(Ar*ug0*Mg(3));
mco = nco./(Ar*ug0*Mg(4));
mh2 = h2./(Ar*ug0*Mg(5));
mn2 = Fint./(Ar*ug0*Mg(6));
mgt = mo2+mh2o+mco2+mco+mh2+mn2;

fo2 = mo2./mgt;
```

```
% ---------------------- Reaction terms ---------------
for i =1:3
Phi(i) = rA*sqrt(k(i)/Ds); % Thiele Modulus (Dimless)
end
% Resistance Terms
a = (Fs/F0s)^(1/3);
r = a*rA;
f = a^3;
U(1) = 1/(Sh*Dg); % Gas film layer resistance
U(2) = (1-a)/(a*Ds); % Ash layer resistance in Unexposed Core
Model
Phi(1) = sqrt(beta)*Phi(1);
for i=1:3
U(3) = 1/(a*Ds*(a*Phi(i)*coth(a*Phi(i))-1)); % Reaction
Resistance
RmT(i) = sum(U);
end
Phi(1) = 1/sqrt(beta)*Phi(1);
for i=1:3
rx(i) = 2/dp*(Fg(i)/(Ar*ug*Mg(i)))/RmT(i);
end

Co2 = Sgn(Fg(1)/(Ar*ug*Mg(1)));
Ch2o = Sgn(Fg(2)/(Ar*ug*Mg(2)));
Cco2 = Sgn(Fg(3)/(Ar*ug*Mg(3)));
Cco = Sgn(Fg(4)/(Ar*ug*Mg(4)));
Ch2 = Sgn(Fg(5)/(Ar*ug*Mg(5)));
rx(4) = k(4)*(Cco*Ch2o - Cco2*Ch2/Keq4);
rx(5) = k(5)/Tg^1.5*Cco*Co2^0.25*Ch2o;
rx(6) = k(6)/Tg^1.5*Ch2^1.5*Co2;
lambda(1) = Co2/Cco2;
lambda(2) = Co2/Cco;
lambda(3) = Ch2o/Cco;
lambda(4) = Cco2/Cco;
rateflux = dydx(r,lambda);

co2rate = -Ds*Cco2/rA*rateflux(1);
corate = -Ds*Cco/rA*rateflux(2);
dAs_dz = Ar*(1-eps)*6/(2*rA)*f;
dVs_dz = Ar*(1-eps)*f;
dVg_dz = Ar*eps;
dFs_c_dz = Ms(1)*(-(rx(1)+rx(2)+rx(3))*dAs_dz);
dFg_o2_dz = Mg(1)*((-beta*rx(1))*dAs_dz + 0.5*(-rx(5)-
rx(6))*dVg_dz);
dFg_h2o_dz = Mg(2)*((-rx(2))*dAs_dz + (-rx(4)+rx(6))*dVg_dz);
dFg_aco2_dz = Mg(3)*(((2*beta-1)*rx(1)-rx(3))*dAs_dz +
(rx(4)+rx(5))*dVg_dz);
dFg_aco_dz = Mg(4)*(((2-2*beta)*rx(1)+rx(2)+2*rx(3))*dAs_dz + (-
rx(4)-rx(5))*dVg_dz);
dFg_h2_dz = Mg(5)*(rx(2)*dAs_dz + (rx(4)-rx(6))*dVg_dz);
dFg_nco2_dz = Mg(3)*((co2rate)*dAs_dz + (rx(4)+2*rx(5))*dVg_dz);
dFg_nco_dz = Mg(4)*((corate)*dAs_dz + (-rx(4)-2*rx(5))*dVg_dz);
dF = [ dFs_c_dz;
```

```
dFg_o2_dz;
dFg_h2o_dz;
dFg_aco2_dz;
dFg_aco_dz;
dFg_h2_dz;
dFg_nco2_dz;
dFg_nco_dz;
dAs_dz;
];
```

3) Rateflux Function (dydx)

```
% Numerical Solution for Concentration Profile in a single coal
particle
% ----------------------------------------------------% Equation
solved:
%

% del^2(y3) = Phi^2*(y3) - C*(y1)
% del^2(y4) = - C1*(y1) - C2*(y2) - C3*(y3)
%
% del: diffential operator in radial coordinate system
% Phi: Theile Modulus

% ------------------------------------------------------
function dydx = dydx(r,lambda)
global rA N1 Phi beta
lambda13 = lambda(1);
lambda14 = lambda(2);
lambda24 = lambda(3);
lambda34 = lambda(4);
n = 101;
a = r/rA;
k = floor(a*(n-1))
del = 1/(n-1);
x = del*(0:n-1);

% ------------------------------------------------------
% Analytical Solution for y1(O2)
Phi(1) = sqrt(beta)*Phi(1);
si1 = 1/(a*Phi(1)*coth(a*Phi(1))-1);
si2 = a*(1/N1-1);
A1 = a/(1+si1+si2);
B1 = 1 - (1/N1-1)*A1;
A2 = a/sinh(a*Phi(1))*(-A1/a+B1);
y1 = zeros(n,1);
y1(1) = A2*Phi(1);
for i = 2:k
y1(i) = A2*(sinh(Phi(1)*x(i))/x(i));
end
for i = k+1:n
y1(i) = -A1/x(i)+B1;
end
```

```
Phi(1) = 1/sqrt(beta)*Phi(1);
% ------------------------------------------------------
% Analytical Solution for y2(H2O)
si1 = 1/(a*Phi(2)*coth(a*Phi(2))-1);
si2 = a*(1/N1-1);
A1 = a/(1+si1+si2);
B1 = 1 - (1/N1-1)*A1;
A2 = a/sinh(a*Phi(2))*(-A1/a+B1);
y2 = zeros(n,1);
y2(1) = A2*Phi(2);
for i = 2:k
y2(i) = A2*(sinh(Phi(2)*x(i))/x(i));
end
for i = k+1:n
y2(i) = -A1/x(i)+B1;
end


% ------------------------------------------------------%
Numerical Solution for y3(CO2)

A = zeros(n,n);
b = zeros(n,1);
coeff = (2*beta-1)*lambda13*(Phi(1)*del)^2;

% Core Region
for i=2:k-1
A(i,i-1) = (1-(Phi(3)*del)^2)*x(i-1)^2;
A(i,i) = -(x(i)^2+x(i-1)^2);
A(i,i+1) = x(i)^2;
b(i) = -coeff*x(i-1)^2*y1(i-1); % Other Reactions term
end

% Ash Region
for i=k+1:n-1
A(i,i-1) = x(i-1)^2;
A(i,i) = -(x(i)^2+x(i-1)^2);
A(i,i+1) = x(i)^2;
b(i) = 0;
end

% Boundary Conditions
% 1. Flux @ center = 0
A(1,1) = 1;
A(1,2) = -1;
b(1) = 0;

% 2. Continuity of flux @ Core-Shell interface
A(k,k-1) = 1;
A(k,k) = -2;
A(k,k+1) = 1;
b(k) = 0;
```

```
% 3. Continuity of flux @ Shell-Gas film interface
A(n,n-1) = -1;
A(n,n) = (1+N1*del);
b(n) = N1*del;
y3 = A\b;

% ------------------------------------------------%

Numerical Solution for y4(CO)
A = zeros(n,n);
b = zeros(n,1);

% Core Region
for i=2:k-1
A(i,i-1) = x(i-1)^2;
A(i,i) = -(x(i)^2+x(i-1)^2);
A(i,i+1) = x(i)^2;
term(1) = -lambda14*y1(i-1)*Phi(1)^2*(2-2*beta);
term(2) = -lambda24*y2(i-1)*Phi(2)^2;
term(3) = -lambda34*y3(i-1)*Phi(3)^2*2;
b(i) = del^2*x(i-1)^2*(sum(term)); % Other Reactions term
end

% Ash Region
for i=k+1:n-1
A(i,i-1) = x(i-1)^2;
A(i,i) = -(x(i)^2+x(i-1)^2);
A(i,i+1) = x(i)^2;
b(i) = 0;
end

% Boundary Conditions
% 1. Flux @ center = 0
A(1,1) = 1;
A(1,2) = -1;
b(1) = 0;

% 2. Continuity of flux @ Core-Shell interface
A(k,k-1) = 1;
A(k,k) = -2;
A(k,k+1) = 1;
b(k) = 0;

% 3. Continuity of flux @ Shell-Gas film interface
A(n,n-1) = -1;
A(n,n) = (1+N1*del);
b(n) = N1*del;
y4 = A\b;

%-------------------------------------------------------
dydx(1) = (y3(n)-y3(n-1))/del;
dydx(2) = (y4(n)-y4(n-1))/del;
```

4) Sign Function

```
% Function to evaluate absolute value or zero.
function Sgn = Sgn(x)
if x > 0
Sgn = x;
else
Sgn = 1e-12;
end
```